Bol. Soc. Paran. Mat.
©SPM – E-ISSN-2175-1188
SPM: www.spm.uem.br/bspm

(3s.) **v. 2026 (44) 3** : 1–17.
ISSN-0037-8712
doi:10.5269/bspm.79640

Optimal Strategies for a Controlled SIR Model with Dynamic Reproduction Number and Economic Feedback

Achraf Bouhmady*, Mustapha Serhani, Nadia Raissi

ABSTRACT: Mathematical models play a critical role in analyzing infectious disease dynamics, yet existing frameworks often overlook the interplay between epidemiological and socio-economic factors. This study develops the SIRKρ model, a novel mathematical framework that integrates time-varying transmission dynamics with economic feedback mechanisms. The model incorporates optimal control theory to determine vaccination v and public health intervention c strategies that simultaneously minimize disease prevalence and economic losses while maintaining the effective reproduction number below unity. Through analytical derivation using Pontryagin's Maximum Principle and numerical validation with Hepatitis B (HBV) parameters, we demonstrate the model's effectiveness in outbreak control. Simulation results show that optimized intervention strategies can reduce HBV infections while supporting economic recovery. The SIRKρ framework provides a comprehensive approach for public health decision-making that balances epidemiological control with economic considerations.

Key Words: Optimal control, SIR model, public health, epidemiology.

Contents

1. Introduction

Mathematical modeling has become an indispensable tool in modern epidemiology, providing crucial insights into disease transmission patterns and the effectiveness of intervention strategies. Since the development of the foundational Susceptible-Infected-Recovered (SIR) model by Kermack and McKendrick, compartmental models have served as the cornerstone for analyzing infectious disease dynamics [17,20]. The versatility of these models has led to numerous extensions addressing various aspects of disease spread, including deterministic formulations [21], stochastic approaches [25], and age-structured variations [19].

* Corresponding author.
2020 *Mathematics Subject Classification:* 92D30, 49J15, 49K15.
Submitted October 19, 2025. Published January 22, 2026

Despite these advancements, significant gaps remain in current modeling frameworks. Traditional epidemiological models often treat key parameters, such as the reproduction number, as static values, ignoring their inherent dynamism in real-world scenarios. Furthermore, while many studies have successfully captured biological aspects of disease transmission, they frequently overlook the crucial interplay between epidemiological processes and socio-economic factors. This limitation becomes particularly apparent when modeling long-term epidemics or designing sustainable intervention strategies, where economic considerations often determine practical implementation feasibility.

Recent research has made important strides in addressing these limitations. Several studies have developed methods for estimating time-varying reproduction numbers [18,29], while others have incorporated economic factors into epidemic models [24]. Advanced modeling techniques, including delay differential equations [30], fractional calculus approaches [5], and stochastic formulations [3], have provided new tools for capturing complex transmission dynamics. In parallel, optimal control theory has emerged as a powerful framework for designing intervention strategies [11], particularly for diseases like Hepatitis B where vaccination plays a crucial role [16].

However, current approaches often treat epidemiological and economic components separately, failing to capture their dynamic interdependence. This separation limits models' ability to inform comprehensive public health strategies that must balance infection control with economic sustainability. Additionally, many existing frameworks lack the flexibility to adapt to changing transmission patterns resulting from behavioral changes or policy interventions, reducing their practical utility for long-term epidemic management.

This study introduces the SIRKρ model, a novel framework that addresses these limitations through three key innovations. First, it incorporates a dynamic reproduction number $\rho(t)$ that responds to both disease prevalence and intervention measures. Second, it explicitly models economic impacts through a dedicated state variable $K(t)$ that tracks both the costs of infection and the benefits of control measures. Third, it integrates these components into an optimal control framework to identify balanced intervention strategies that simultaneously minimize disease burden and economic losses while preventing future outbreaks through reproduction number control.

Control theory offers several complementary approaches for analyzing and designing dynamic decision systems. Recent advances include multi-objective formulations that characterize trade-offs between conflicting sustainability goals through Pareto-efficient control [7], and viability-based approaches that maintain system trajectories within safety or feasibility domains over time [4]. These perspectives demonstrate the flexibility of control theory tools for addressing coupled bioeconomic and ecological processes. In the present work, our aim is not to explore Pareto frontiers or viability kernels but to determine time-dependent control functions that minimize a single objective functional representing the combined epidemiological and economic burden. For such maximization or minimization settings, the Pontryagin Maximum Principle (PMP) provides the natural analytical framework, allowing us to derive necessary optimality conditions and characterize the structure of optimal intervention strategies.

We formulate this as an optimal control problem with vaccination rate $v(t)$ and public health intervention intensity $c(t)$ as control variables. Our analytical approach employs Pontryagin's Maximum Principle [8,22], a well-established method for solving such dynamic optimization problems [2,28,6]. This methodology has proven particularly effective in epidemiological applications, from outbreak containment [10] to vaccine deployment optimization [23]. We complement our theoretical analysis with numerical simulations using Hepatitis B (HBV) parameters, demonstrating the model's practical utility for public health decision-making.

The paper is organized as follows. Section 2 presents the complete SIRKρ model formulation and its biological rationale. Section 3 conducts a thorough dynamical analysis, establishing fundamental properties such as solution positivity and disease-free equilibria. Section 4 develops the optimal control framework and derives characterization theorems for intervention strategies. Finally, Section 5 presents numerical results and discusses their implications for HBV control policy, followed by conclusions and future research directions.

2. Mathematical Model Description

In epidemiological modeling, compartmental systems are fundamental for analyzing the transmission dynamics of infectious diseases. In this section, we propose an extended SIR model that includes two additional features: a time-dependent effective reproduction number ρ and an economic impact variable K. The resulting framework, referred to as the SIRKρ model, integrates both biological and socio-economic dimensions of disease spread and control. The population is divided into three epidemiological compartments: susceptible $S(t)$, infected $I(t)$, and recovered $R(t)$. The force of infection is governed by a modified incidence term $\rho(t) \cdot \gamma \frac{SI}{N}$, where γ is a scaling factor, and N is the total population ($N(t) = S(t) + R(t) + I(t)$). The variable $\rho(t)$ denotes the effective reproduction number at time t, evolving dynamically in response to epidemic pressure and interventions.

A visual summary of the model's structure and interactions among compartments, control functions,

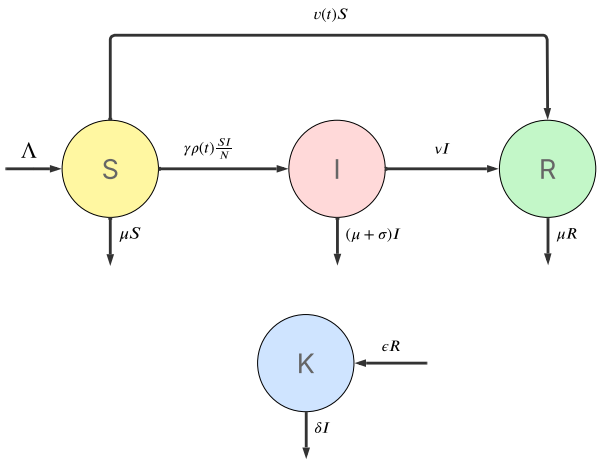

Figure 1: Workflow diagram of the generalized SIRKρ epidemic model.

and the economic state is provided in Fig. 1.

The model is defined by the following system of differential equations over the time interval $[0, T]$.

$$\begin{cases} \dfrac{dS}{dt} = \Lambda - \rho \cdot \gamma \dfrac{SI}{N} - (\mu + v)S, \\ \dfrac{dI}{dt} = \rho \cdot \gamma \dfrac{SI}{N} - (\mu + \nu + \sigma)I, \\ \dfrac{dR}{dt} = vS + \nu I - \mu R, \\ \dfrac{d\rho}{dt} = \eta - kI - \alpha(\rho - \rho_0) - \beta_v v - \beta_c c, \\ \dfrac{dK}{dt} = -\delta I + \epsilon R, \\ S(0) = S_0, \quad I(0) = I_0, \quad R(0) = R_0, \quad \rho(0) = \rho_0, \quad K(0) = K_0. \end{cases} \tag{2.1}$$

All parameters are strictly positive: $\Lambda, \mu, \gamma, \nu, \sigma, \eta, k, \alpha, \beta_v, \beta_c, \delta, \epsilon > 0$, and the initial condition $x_0 = (S_0, I_0, R_0, \rho_0, K_0)$ lies in $\mathbb{R}^5_+$. In this system, Λ represents the recruitment rate into the susceptible class, while μ denotes the natural death rate. The time-dependent vaccination policy v transfers individuals from the susceptible to the recovered compartment. Parameters ν and σ correspond to recovery and disease-induced mortality rates, respectively, making $\mu + \nu + \sigma$ the total outflow rate from the infected class. The scaling parameter γ relates the reproduction number to transmission dynamics.

The effective reproduction number ρ is modeled as a dynamic state variable. The term $-kI$ captures adaptive behavioral responses [15]. Reversion to the baseline ρ_0 is governed by $-\alpha(\rho(t) - \rho_0)$, reflecting

the tendency for transmission to normalize when interventions are relaxed. The parameter η represents a baseline level of behavioral activation (e.g., sustained public awareness or social norms) that maintains a non-zero response in ρ even without infections, accounting for societal influences independent of prevalence [9,27]. Vaccination v and public health interventions c reduce transmission through the terms $-\beta_v v$ and $-\beta_c c$, respectively, capturing effects of immunization and altered risk perception [1,12]. The function c encodes non-pharmaceutical interventions such as lockdowns, mobility restrictions, and mask mandates [13].

The economic state variable K quantifies societal burden, where $-\delta I$ represents economic losses from healthcare costs and lost productivity, while ϵR models economic gains from workforce reentry and societal stabilization. The parameters k, δ, and ϵ are socio-economic in nature: k governs responsiveness to infection prevalence, δ quantifies per capita infection costs, and ϵ reflects recovery strength through immunity.

The primary objective is to control the system in order to reduce viral spread by minimizing infections. To achieve this, we first conduct a qualitative analysis of the uncontrolled system to examine its behavior around critical points.

3. Dynamical Analysis of the Model

This section investigates the qualitative behavior of the model. We assume constant control measures $v(t) \equiv v \in [0, v_{max}]$ (vaccination rate) and $c(t) \equiv c \in [0, c_{max}]$ (public health intervention). Here, $v_{max} > 0$ is the maximal feasible vaccination rate (limited by logistics and supply), and $c_{max} \in (0, 1]$ is the maximal attainable intensity of non-pharmaceutical interventions.
The system (2.1) admits a dynamical reduction to the (S, I, R, ρ)-subsystem through structural decoupling, $K(t)$ functioning as output variable. The essential dynamics are captured by:

$$\begin{cases} \dfrac{dS}{dt} = \Lambda - \rho \cdot \gamma \dfrac{SI}{N} - (\mu + v)S, \\ \dfrac{dI}{dt} = \rho \cdot \gamma \dfrac{SI}{N} - (\mu + \nu + \sigma)I, \\ \dfrac{dR}{dt} = vS + \nu I - \mu R, \\ \dfrac{d\rho}{dt} = \eta - kI - \alpha(\rho - \rho_0) - \beta_v v - \beta_c c, \\ S(0) = S_0, \quad I(0) = I_0, \quad R(0) = R_0, \quad \rho(0) = \rho_0. \end{cases} \tag{3.1}$$

The economic variable evolves as

$$K(t) = K_0 + \int_0^t (-\delta I(\tau) + \epsilon R(\tau))\, d\tau.$$

The model's plausibility is established through the following invariant region result.
The model's plausibility is established through proving the positivity and boundedness of trajectories.

Proposition 3.1 *Consider $x = (S, I, R, \rho)$ a trajectory of the system (3.1), starting at $\mathbf{x}_0 = (S_0, I_0, R_0, \rho_0)$. If $(S_0, I_0, R_0) \in \mathbb{R}^3_+$, then $(S(t), I(t), R(t)) \in \mathbb{R}^3_+$, $\forall\, t \geq 0$.*

Proof: From the first differential equation in the system (3.1), we get

$$\frac{dS}{dt} \geq (-\rho \cdot \gamma \frac{I}{N} - (\mu + v))S.$$

Hence, using standards arguments of differential inequalities, it derives that

$$S \geq S_0 exp\left(\int_0^t -\rho(r) \cdot \gamma \frac{I(r)}{N(r)} dr - (\mu + v)t\right).$$

So, S is non negative as soon as S_0 is too.
The same arguments can be applied to the second equation of the vector field to prove that $I \geq 0$.
For the third $R-$equation, since S and I are nonnegative, we obtain that

$$\frac{dR}{dt} \geq -\mu R,$$

which lead to

$$R \geq R_0 e^{-\mu t}.$$

then, R is non negative since R_0 is too. □

In the next proposition, we establish the boundedness of trajectories and accordingly, the positivity of ρ.
Assume that

$$\eta > k\frac{\Lambda}{\mu} + \beta(v_{max} + c_{max}) - \alpha\rho_0, \tag{3.2}$$

where $\beta = max(\beta_v; \beta_c)$. We define the set Γ as:

$$\Gamma = \left\{ (S, I, R, \rho) \in \mathbb{R}^4_+ \;\middle|\; S + I + R \leq \frac{\Lambda}{\mu},\ \rho \in [\rho_{\min}, \rho_{\max}] \right\}$$

where $\rho_{\min} = \rho_0 + \frac{\eta - k\frac{\Lambda}{\mu} - \beta_v v - \beta_c c}{\alpha}$, and $\rho_{\max} = \rho_0 + \frac{\eta - \beta_v v - \beta_c c}{\alpha}$.

Proposition 3.2 *Consider $x = (S, I, R, \rho)$ a trajectory of the system (3.1), starting at $\mathbf{x}_0 = (S_0, I_0, R_0, \rho_0)$. If $\mathbf{x}_0 \in \Gamma$, then $\mathbf{x}(t) \in \Gamma$, $\forall t \geq 0$.*

Proof: The proof establishes three key properties: boundedness of the total population, confinement of the reproduction number, and its non-negativity.
For the total population $N = S + I + R$, the summation of the first three equations of the reduced system (3.1) yields

$$\begin{aligned} \frac{dN}{dt} &= \Lambda - \mu N - \sigma I, \\ &\leq \Lambda - \mu N. \end{aligned} \tag{3.3}$$

Application of Gronwall's inequality demonstrates that

$$N(t) \leq \frac{\Lambda}{\mu} + \left(N_0 - \frac{\Lambda}{\mu} \right) e^{-\mu t}, \tag{3.4}$$

confirming that if $N_0 \in \Gamma$, then $N(t) \in \Gamma$, $\forall \geq 0$.
For the reproduction number, from the ρ-equation in the dynamical system (3.1), it follows that

$$\frac{d\rho}{dt} \leq -\alpha\rho + \eta + \alpha\rho_0 - (\beta_v v + \beta_c c).$$

It emerges that

$$\rho(t) \leq \rho_{\max} + (\rho_0 - \rho_{max}) e^{-\alpha t},$$

with $\rho_{\max} = \rho_0 + \frac{\eta - \beta_v v - \beta_c c}{\alpha}$.
Since $\rho_0 \leq \rho_{max}$, we get

$$\rho(t) \leq \rho_{\max}.$$

The lower bound follows similarly by considering the worst-case infection prevalence and the inequality (3.4),

$$I \leq N \leq \frac{\Lambda}{\mu},$$

yielding

$$\rho(t) \geq \rho_{\min} = \rho_0 + \frac{\eta - k\frac{\Lambda}{\mu} - \beta_v v - \beta_c c}{\alpha}.$$

We achieve the proof by remarking that according to assumption (3.2), $\rho_{min} \geq 0$ and by the way

$$\rho(t) \geq 0, \ \forall t \geq 0.$$

□

3.1. Stability Analysis

Consider the reduced epidemiological system (3.1) with feasible region Γ. We restrict ourselves to analyzing the stability of the disease-free equilibrium, since our aim consists in proving that this equilibrium is only locally stable if the effective reproduction number is lower than 1. This fact justifies the use of optimal control to eradicate the pandemic. But, there exists an endemic equilibrium which we will prove the existence and uniqueness in the appendix A. By setting the right-hand sides of the system to zero and assuming $I = 0$, we obtain the disease-free equilibrium (DFE) point:

$$\mathcal{E}_0 = (S^*, I^*, R^*, \rho^*) = \left(\frac{\Lambda}{\mu + v}, \ 0, \ \frac{v}{\mu} \cdot \frac{\Lambda}{\mu + v}, \ \rho_0 + \frac{\eta - \beta_v v - \beta_c c}{\alpha} \right).$$

To examine the local stability of $\mathcal{E}_0$, we define the effective reproduction number, denoted $\mathcal{R}_{\text{eff}}$, given by:

$$\mathcal{R}_{\text{eff}} = \rho \cdot \frac{\gamma}{\mu + \nu + \sigma} \cdot \frac{S}{N}.$$

At the DFE, we have $S = S^*$, $R = R^*$, and $N = S^* + R^*$, yielding:

$$\mathcal{R}_{\text{DFE}} := \mathcal{R}_{\text{eff}}(\mathcal{E}_0) = \frac{\gamma}{\mu + \nu + \sigma} \left(\rho_0 + \frac{\eta - \beta_v v - \beta_c c}{\alpha} \right) \cdot \frac{S^*}{S^* + R^*}.$$

This quantity characterizes the potential of disease invasion in a population where vaccination may create a positive recovered class even in the absence of infection.

Theorem 3.1 *The disease-free equilibrium $\mathcal{E}_0$ of the system (3.1) is locally asymptotically stable (LAS) if and only if $\mathcal{R}_{\text{DFE}} < 1$.*

Proof: The Jacobian matrix at $\mathcal{E}_0$ is:

$$J(\mathcal{E}_0) = \begin{pmatrix} -(\mu + v) & -\gamma \left(\rho_0 + \frac{\eta - \beta_v v - \beta_c c}{\alpha} \right) \frac{S^*}{N^*} & 0 & 0 \\ 0 & \gamma \left(\rho_0 + \frac{\eta - \beta_v v - \beta_c c}{\alpha} \right) \frac{S^*}{N^*} - (\mu + \nu + \sigma) & 0 & 0 \\ v & \nu & -\mu & 0 \\ 0 & -k & 0 & -\alpha \end{pmatrix}.$$

The eigenvalues are:

$$\lambda_1 = -(\mu + v), \quad \lambda_2 = -\mu, \quad \lambda_3 = (\mu + \nu + \sigma)(\mathcal{R}_{\text{DFE}} - 1), \quad \lambda_4 = -\alpha.$$

It follows that $\mathcal{E}_0$ is locally asymptotically stable if all eigenvalues are negative, i.e., if and only if $\mathcal{R}_{\text{DFE}} < 1$. Conversely, if $\mathcal{R}_{\text{DFE}} > 1$, then $\lambda_3 > 0$, and the equilibrium is a saddle point. □

The preceding stability analysis establishes a critical threshold: when the basic reproduction number $\mathcal{R}_{\text{DFE}} < 1$, the disease is expected to die out. Conversely, if $\mathcal{R}_{\text{DFE}} > 1$, the disease-free equilibrium becomes unstable, creating the potential for a sustained endemic state.

However, this equilibrium-based analysis has practical limitations. It does not address the transient disease burden during an outbreak, nor does it provide a strategy for optimally allocating limited resources

(e.g., vaccines, public health campaigns) over time to minimize both epidemiological and socioeconomic costs.

To address these dynamic challenges, we turn to optimal control theory. Our goal is to design time-dependent intervention strategies, namely vaccination $v(t)$ and public awareness campaigns $c(t)$, that actively steer the epidemic's trajectory. This framework allows us to find a balance between mitigating the infection and managing the costs of intervention.

4. Optimal Control Problem (OCP)

We formulate time-dependent control strategies that minimize both disease prevalence and intervention costs over a finite horizon T. The control vector $\mathbf{u}(t) = (v(t), c(t))$, comprises the vaccination rate $v(t)$ and public health intervention intensity $c(t)$, where the admissible set

$$\mathcal{U}_{\text{ad}} = \left\{ \mathbf{u} = (\mathbf{v}, \mathbf{c}) \in L^2([0,T]; \mathbb{R}^2) \;\middle|\; (\mathbf{v}(t), \mathbf{c}(t)) \in \mathbb{U},\ \forall t \in [0,T]. \right\},$$

where $\mathbb{U} = [0, v_{max}] \times [0, c_{max}]$.

The cost functional combines epidemiological and economic effects. It penalizes large numbers of infections, deviations of the economic indicator from its benchmark K_{target}, and excessive use of interventions.
Here $K_{\text{target}} > 0$ represents the desired economic level (e.g., pre-epidemic baseline or a normalized target such as 100). The running cost is

$$\int_0^T \left[w_I I(t)^2 + w_K (K(t) - K_{\text{target}})^2 + w_v v(t)^2 + w_c c(t)^2 \right] dt,$$

where $w_I, w_K, w_v, w_c > 0$ are weighting parameters reflecting the relative importance of each term.

A crucial epidemiological constraint is that the reproduction number $\rho(T)$ remains below a critical threshold ρ_{crit} at T. Enforcing this ensures the epidemic does not grow uncontrollably, keeping the number of secondary infections per case at a manageable level:

$$\rho(T) \leq \rho_{\text{crit}}.$$

The OCP is formulated as:

$$\min_{\mathbf{u}(\cdot) \in \mathcal{U}_{\text{ad}}} \quad J(\mathbf{u}) = \int_0^T \left[w_I I(t)^2 + w_K (K(t) - K_{\text{target}})^2 + w_v v(t)^2 + w_c c(t)^2 \right] dt \tag{4.1}$$

subject to:

$$\begin{cases} \dfrac{dS}{dt} = \Lambda - \rho \cdot \gamma \dfrac{SI}{N} - (\mu + v)S, \\ \dfrac{dI}{dt} = \rho \cdot \gamma \dfrac{SI}{N} - (\mu + \nu + \sigma)I, \\ \dfrac{dR}{dt} = vS + \nu I - \mu R, \\ \dfrac{d\rho}{dt} = \eta - kI - \alpha(\rho - \rho_0) - \beta_v v - \beta_c c, \\ \dfrac{dK}{dt} = -\delta I + \epsilon R, \\ \mathbf{x}(0) = \mathbf{x}_0, \\ \rho(T) \leq \rho_{\text{crit}}. \end{cases} \tag{4.2}$$

4.1. Existence of an Optimal Solution

To ensure that an optimal solution exists for the control problem, we first define the system dynamics explicitly. The evolution of the state variables $\mathbf{x}(t) = (S(t), I(t), R(t), \rho(t), K(t))$ is governed by the vector field $f(x, u)$, which represents the time derivatives of the states under the influence of the control variable $\mathbf{u} = (\mathbf{v}, \mathbf{c}) \in \mathcal{U}_{\text{ad}}$. The vector field $f(x, u)$ is defined, for $x = (S, I, R, \rho, K) \in \Gamma$ and $u = (v, c) \in \mathbb{U}$, as

$$f(x,u) = \begin{pmatrix} \Lambda - \rho \cdot \gamma \frac{SI}{N} - (\mu + v)S, \\ \rho \cdot \gamma \frac{SI}{N} - (\mu + \nu + \sigma)I, \\ vS + \nu I - \mu R, \\ \eta - kI - \alpha(\rho - \rho_0) - \beta_v v - \beta_c c, \\ -\delta I + \epsilon R \end{pmatrix}.$$

Assume that

$$\frac{\eta - \alpha(\rho_{crit} - \rho_0)}{\min(\beta_v, \beta_c)} \leq v_{max} + c_{max}. \tag{4.3}$$

Proposition 4.1 (Existence of an optimal control) *The optimal control problem (4.1) -(4.2) admits at least one optimal solution.*

Proof: In the first part, we prove that the dynamical system (4.2) admits a unique solution $\mathbf{x}(\cdot) = (S(\cdot), I(\cdot), R(\cdot), \rho(\cdot), K(\cdot))$, for each control $\mathbf{u} = (\mathbf{v}, \mathbf{c}) \in \mathcal{U}_{\text{ad}}$. Indeed, the dynamic $f(x, u)$, for $(x, u) \in \Gamma \times \mathbb{U}$, is continuously differentiable, C^1, this regularity follows from the structure of the system ensuring smoothness in both state and control variables. Moreover, the dynamics f satisfy the linear growth condition. To show this, we must prove that there exists a constant $C > 0$ such that $\|f(x, u)\| \leq C(1 + \|x\|)$, for each $(x, u) \in \Gamma \times \mathbb{U}$.
Using the positivity and boundedness of S, I, R, as proven in propositions (3.1) - (3.2), and the boundedness of the control values v, c, we get for each component $|f_i|$, with $i = 1, \cdots, 5$, and $x = (S, I, R, \rho, K) \in \Gamma$, $u = (v, c) \in \mathbb{U}$

$$\begin{aligned}
|f_1(x,u)| &\leq \Lambda + \gamma\rho\frac{S}{N}I + (\mu + v_{max})S; \\
&\leq \Lambda + \gamma N_{max}\rho + (\mu + v_{max})N_{max}, \\
|f_2(x,u)| &\leq \gamma\rho\frac{S}{N}I + (\mu + \nu + \sigma)I; \\
&\leq \gamma N_{max}\rho + (\mu + \nu + \sigma)N_{max}, \\
|f_3(x,u)| &\leq (v_{max} + \nu + \mu)N_{max}, \\
|f_4(x,u)| &\leq \eta + kI + \alpha\rho + \alpha\rho_0 + \beta_v v_{max} + \beta_c c_{max}; \\
&\leq \eta + kN_{max} + \alpha\rho + \alpha\rho_0 + \beta_v v_{max} + \beta_c c_{max}, \\
|f_5(x,u)| &\leq \delta I + \epsilon R; \\
&\leq (\delta + \epsilon)N_{max},
\end{aligned}$$

where N_{max} is the upper bound of $N = S + I + R$.
Summing these inequalities leads to

$$\|fx, u)\|_1 \leq C_1 + C_2\rho,$$

where $C_1 = \Lambda + (3\mu + 2v_{max} + 2\nu + \sigma + k + \delta + \epsilon)N_{max} + \eta + \alpha\rho_0 + \beta_v v_{max} + \beta_c c_{max}$, and $C_2 = 2\gamma N_{max} + \alpha$. Since $\rho \leq \|x\|_1$, then we get

$$\|f(x,u)\|_1 \leq C(1 + \|x\|_1),$$

where $C = \max\{C_1, C_2\}$. Thus, the function f satisfies the linear growth condition.
It derives from these features that the dynamical system (4.1), without terminal constraint $\rho(T) \leq \rho_{\text{crit}}$, admit a unique solution $\mathbf{x}(\cdot)$ for each control pair $\mathbf{u} = (\mathbf{v}, \mathbf{c}) \in \mathcal{U}_{\text{ad}}$.

To take into account on this final constraint, we must prove that the system is controllable, that is, there exist a control pairs $\mathbf{u} = (\mathbf{v}, \mathbf{c}) \in \mathcal{U}_{\text{ad}}$, generating a trajectory $\mathbf{x}(\cdot) = (S(\cdot), I(\cdot), R(\cdot), \rho(\cdot), K(\cdot))$,

fulfilling $\rho(T) \leq \rho_{\text{crit}}$.
The assumption (4.3) implies that there exists $u = (v, c) \in \mathbb{U}$ such that

$$\frac{\eta - \alpha(\rho_{\text{critic}} - \rho_0)}{\min(\beta_v, \beta_c)} \leq v + c \leq v_{\max} + c_{\max},$$

which implies that

$$\begin{aligned} \eta - \alpha(\rho_{\text{critic}} - \rho_0) \leq & \quad \min(\beta_v, \beta_c)(v + c), \\ \leq & \quad \beta_v v + \beta_c c. \end{aligned} \tag{4.4}$$

It follows that

$$\rho_0 + \frac{\eta - (\beta_v v + \beta_c c)}{\alpha} \leq \rho_{\text{crit}}.$$

So,

$$\rho_{\max} < \rho_{\text{crit}}.$$

On the other hand, according to the proposition (3.2), since $\rho \leq \rho_{\max}$, we conclude the existence of $u = (v, c) \in \mathbb{U}$ such that $\rho(T) \leq \rho_{\max}$, which implies that

$$\rho(T) \leq \rho_{\text{crit}},$$

indicating that the terminal constraint is satisfied.
Therefore we establish the existence of a control $\mathbf{u} = (\mathbf{v}, \mathbf{c}) \in \mathcal{U}_{\text{ad}}$, with $\mathbf{u}(t) = u$, for all $t \in [0, T]$ such that the system (4.2) admits a unique solution fulfilling the terminal constraint, and consequently ensuring the controllability.

The second part concerns the existence of an optimal control of the problem (4.1) - (4.2). For this, we invoke [Theorem 6.2.1 in [26]].
Since $\mathbb{U}$ is compact, we can demonstrate through standard arguments that $\mathcal{U}_{\text{ad}}$ is also compact. Furthermore, the cost functional is given by

$$J(\mathbf{u}) = \int_0^T f_0(\mathbf{x}(t), \mathbf{u}(t))\, dt,$$

where

$$f_0(x, u) = w_I I^2 + w_K (K - K_{\text{target}})^2 + w_v v^2 + w_c c^2.$$

The function f_0 is convex with respect to u, as it is a positive weighted sum of the quadratic functions.

We must now establish that the set

$$\widetilde{V}(t, \mathbf{x}) = \left\{ (f(x, u), f_0(x, u) + \xi) \in \mathbb{R}^5 \times \mathbb{R} \,\middle|\, u \in \mathbb{U},\, \xi > 0 \right\}.$$

is convex for each $(t, x) \in [0, T] \times \mathbb{R}^5$. Since f is affine in u and f_0 is convex in u, the mapping $u \mapsto (f(x, u), f_0(x, u) + \xi$ is convex for every fixed (t, x) and $\xi > 0$. Consequently, the set $\widetilde{V}(t, x)$ is convex for all (t, x).

Moreover, by Proposition (3.2), all trajectories starting from the feasible initial conditions remain bounded for all $t \in [0, T]$. In particular, there exists a constant $b > 0$ such that, for every admissible control $\mathbf{u} \in \mathcal{U}_{\text{ad}}$,

$$\sup_{t \in [0,T]} (\|\mathbf{x}(t)\| + T) \leq b.$$

Thus, the solutions are uniformly bounded over time.

Since all hypotheses of Theorem 6.2.1 in [26] are satisfied, we conclude that there exists at least one optimal control $\mathbf{u}^*(\cdot) \in \mathcal{U}_{\text{ad}}$ minimizing the cost functional $J(\mathbf{u})$ while satisfying the system dynamics and the state constraints.

□

4.2. Features of optimal control

Let $\mathcal{H}$ be the Hamiltonian corresponding to the optimal control problem (4.1-4.2):

$$\mathcal{H} : \mathbb{R}^5 \times \mathbb{R}^5 \times \mathbb{U} \to \mathbb{R}, \quad (\boldsymbol{\xi}, \boldsymbol{\lambda}, u) \mapsto \mathcal{H}(\boldsymbol{\xi}, \boldsymbol{\lambda}, u) = L(\boldsymbol{\xi}, u) + \langle \boldsymbol{\lambda}, f(\boldsymbol{\xi}, u) \rangle,$$

where $\boldsymbol{\xi} = (S, I, R, \rho, K)^\top$ is the state vector, $\boldsymbol{\lambda} = (\lambda_S, \lambda_I, \lambda_R, \lambda_\rho, \lambda_K)^\top$ is the adjoint vector, and $u = (v, c)^\top \in \mathbb{U} \subset \mathbb{R}^2$ is the control value. The associated control function is denoted $\mathbf{u}(t) = (v(t), c(t))$.

According to Pontryagin's Maximum Principle [8,22], there exists an absolutely continuous adjoint function $\boldsymbol{\lambda}(t) = (\lambda_S(t), \lambda_I(t), \lambda_R(t), \lambda_\rho(t), \lambda_K(t))^\top$, defined on $[0, T]$, such that the following necessary conditions hold almost everywhere:

$$\dot{\boldsymbol{\xi}}(t) = \frac{\partial \mathcal{H}}{\partial \boldsymbol{\lambda}} \left(\boldsymbol{\xi}(t), \boldsymbol{\lambda}(t), \mathbf{u}(t) \right), \tag{4.5}$$

$$\dot{\boldsymbol{\lambda}}(t) = -\frac{\partial \mathcal{H}}{\partial \boldsymbol{\xi}} \left(\boldsymbol{\xi}(t), \boldsymbol{\lambda}(t), \mathbf{u}(t) \right), \tag{4.6}$$

$$\mathcal{H}(\boldsymbol{\xi}(t), \boldsymbol{\lambda}(t), \mathbf{u}(t)) = \max_{u \in \mathbb{U}} \mathcal{H}(\boldsymbol{\xi}(t), \boldsymbol{\lambda}(t), u), \tag{4.7}$$

$$\boldsymbol{\lambda}(T) \in N_M(\boldsymbol{\xi}(T)), \tag{4.8}$$

where $M = \left\{ \boldsymbol{\xi} \in \mathbb{R}^5 \mid \rho \leq \rho_{\text{crit}} \right\}$ and $N_M(\boldsymbol{\xi}(T))$ denotes the **normal cone** to M at $\boldsymbol{\xi}(T)$. This cone is reduced to zero when the constraint is inactive, that is $\rho(T) < \rho_{\text{crit}}$. However, when the constraint is active, $\rho(T) = \rho_{\text{crit}}$, the normal cone is explicitly given by

$$N_M(\boldsymbol{\xi}(T)) = \left\{ (0, 0, 0, \nu, 0)^\top \mid \nu \geq 0 \right\}.$$

This leads to the following **complementarity condition**:

$$\lambda_\rho(T) \cdot (\rho(T) - \rho_{\text{crit}}) = 0, \quad \lambda_\rho(T) \geq 0.$$

Therefore for,

$$\begin{aligned}
\mathcal{H}(\boldsymbol{\xi}, \boldsymbol{\lambda}, u) = {} & w_I I^2 + w_K (K - K_{\text{target}})^2 + w_v v^2 + w_c c^2 \\
& + \lambda_S \left[\Lambda - \rho\gamma \frac{SI}{N} - (\mu + v) S \right] \\
& + \lambda_I \left[\rho\gamma \frac{SI}{N} - (\mu + \nu + \sigma) I \right] \\
& + \lambda_R \left[vS + \nu I - \mu R \right] \\
& + \lambda_\rho \left[\eta - kI - \alpha(\rho - \rho_0) - \beta_v v - \beta_c c \right] \\
& + \lambda_K \left[-\delta I + \epsilon R \right].
\end{aligned}$$

The adjoint vector λ evolves according to the following system:

$$\begin{aligned}
\dot{\lambda}_S &= \lambda_S \left(\rho\gamma \frac{I}{N} + \mu + v \right) - \lambda_I \rho\gamma \frac{I}{N} - \lambda_R v, \\
\dot{\lambda}_I &= -2 w_I I + \lambda_S \rho\gamma \frac{S}{N} - \lambda_I \left(\rho\gamma \frac{S}{N} - (\mu + \nu + \sigma) \right) - \lambda_R \nu + \lambda_\rho k + \lambda_K \delta, \\
\dot{\lambda}_R &= \mu \lambda_R - \epsilon \lambda_K, \\
\dot{\lambda}_\rho &= -\lambda_S \gamma \frac{SI}{N} + \lambda_I \gamma \frac{SI}{N} + \alpha \lambda_\rho + \epsilon \lambda_K, \\
\dot{\lambda}_K &= -2 w_K (K - K_{\text{target}}),
\end{aligned}$$

with transversality conditions:

$$\lambda_S(T) = 0, \quad \lambda_I(T) = 0, \quad \lambda_R(T) = 0, \quad \lambda_K(T) = 0, \quad \lambda_\rho(T) \geq 0 \quad \text{and} \quad \lambda_\rho(T).(\rho(T) - \rho_{\text{crit}}) = 0.$$

The maximization condition (4.7) yields the optimal control function $\mathbf{u}^*(t) = (v^*(t), c^*(t))$, where $v^*(t)$ and $c^*(t)$ are obtained by minimizing $\mathcal{H}$ with respect to the control values v and c.

$$v^*(t) = \min\left(\max\left(\frac{(\lambda_S - \lambda_R)S - \beta_v \lambda_\rho}{2w_v}, 0\right), v_{\max}\right),$$
$$c^*(t) = \min\left(\max\left(\frac{-\beta_c \lambda_\rho}{2w_c}, 0\right), c_{\max}\right).$$

Thus, the optimal control function is $\mathbf{u}^*(t) = (v^*(t), c^*(t))$.

This structure ensures continuous adaptation to evolving epidemiological conditions. The temporal evolution of optimal strategies occurs in distinct phases. Outbreak suppression requires near-maximal public health intervention ($c^* \approx c_{\max}$) to quickly lower transmission rates. As the number of susceptible population individuals decreases, vaccination efforts progressively increase by v^*. When terminal constraints $\rho(T) \leq \rho_{\text{crit}}$ is applied, the controls often intensify in the final phase to achieve epidemiological targets. The economic trade-off appears through the adjoint variable $\lambda_K(t)$, which measures marginal economic costs as shown in the relation equation:

$$\dot{\lambda}_K = -2w_K(K(t) - K_{\text{target}}). \tag{4.9}$$

Negative values of λ_K resulting from economic shortfalls ($K(t) < K_{\text{target}}$) automatically temper intervention intensity, balancing epidemiological benefits. These controls interact through complementary mechanisms: vaccination induces durable protection via $S \to R$ transitions while public health measures reduce transient transmission.

The next section demonstrates how these principles apply to HBV scenarios, revealing the complex relationship between control effectiveness, economic impact, and implementation constraints that influence optimal policy design.

5. Numerical Simulation: Analysis of Intervention Strategies

We employ direct numerical optimization to solve the optimal control problem (OCP) formulated in Section 4 and evaluate intervention strategies. Our Python-based framework utilizes robust scientific computing tools, including *SciPy*, *CasADi*, and the *IPOPT* solver, which is particularly effective for nonlinear optimization problems arising from OCPs.

The continuous-time OCP is discretized into a finite-dimensional nonlinear programming (NLP) problem using state and control variable discretization. We implement a Crank-Nicolson time integration scheme for this purpose, ensuring both numerical stability and accuracy. Table 1 summarizes the key numerical configuration details, including discretization parameters and solver settings.

For our simulations, we use epidemiological parameters derived from HBV (Hepatitis B Virus) transmission dynamics [19], complemented by economic parameters representing a realistic scenario (see Table 2). We acknowledge that the classic SIR model is a simplification of HBV transmission, as it does not explicitly account for the chronic carrier state, a key feature of the disease.

However, the primary objective of this study is not to create a definitive predictive model for HBV, but rather to introduce and demonstrate a novel optimal control framework that integrates dynamic economic feedback (the K variable) with a time-varying reproduction number (the ρ variable). The foundational SIR structure provides a clear, tractable, and well-understood baseline to rigorously analyze the dynamics of this new methodology. This approach allows us to illustrate the core principles of balancing public health outcomes with economic considerations effectively. This work therefore serves as a proof-of-concept, and the SIRKρ framework developed here can be extended in future research to more complex, disease-specific models (e.g., SEICR) that incorporate features like chronic infection.

The vaccination rate $v_{\max} + c_{max} = 1.5$ satisfies the existence condition from Proposition 4.1. Thus, the theoretical existence guarantee holds for our simulations. The empirical results in Fig. 3 confirm this, showing $\rho(t)$ remains controlled without exceeding implementable vaccination rates.

Table 1: Numerical Configuration for Optimal Control Simulations

Category	**Metric**	**Value**
Solver	NLP Solver	Ipopt (Interior Point Optimizer)
Discretization	Method	Crank-Nicolson Scheme
Precision	Tolerance	10^{-8}
Grid	Time Steps	1000

Table 2: Model Parameters

Parameter	**Description**	**Value**
Λ	Recruitment rate	2.5
μ	Natural death rate	0.013
γ	Transmission rate	0.25
ν	Recovery rate	0.1
σ	Disease-induced mortality rate	0.05
z	Feedback on ρ from infections	0.02
α	Return rate to ρ_0	0.15
ρ_0	Basic reproduction number	4.0
β_v	Vaccination effectiveness	0.7
β_c	Control effectiveness	0.7
η	Behavioral feedback on ρ	0.4
k	Infection feedback scaling	0.002
δ	Economic loss factor	0.1
ϵ	Economic recovery via ρ	0.08
K_{target}	Target economy level	100
ρ_{crit}	Critical ρ threshold	1.0
w_I	Weight on infection minimization	1.0
w_K	Weight on economy preservation	0.3
w_v	Weight on vaccination effort	0.2
w_c	Weight on control effort	0.2
$v_{\max}$	Max vaccination rate	0.8
$c_{\max}$	Max public health intervention	0.7
N	Total population size	100
T	Time horizon (years)	20

5.1. Infection Dynamics and Control Interventions

Simulation results shown in Fig. 2 demonstrate that the implementation of control strategies leads to a substantial reduction in infection levels. Specifically, the controlled intervention reduced infections by approximately 60% compared to the baseline scenario without intervention. The intensive control phase, implemented early in the outbreak, had the most significant impact. Following the peak, a relaxed control phase was introduced to reduce intervention-related costs while maintaining epidemic suppression.

5.2. Reproduction Number and Control Effectiveness

The dynamics of the effective reproduction number, denoted as $\rho(t)$, highlight the success of early and sustained intervention. The simulation in Fig. 3 shows that ρ drops below the critical threshold of 1.0 by year 8 under the optimized strategy. This reduction is primarily due to the early implementation of high-intensity control measures. Furthermore, the vaccination phase plays a key role in preventing resurgence, ensuring that ρ remains below 1.0 throughout the simulation period.

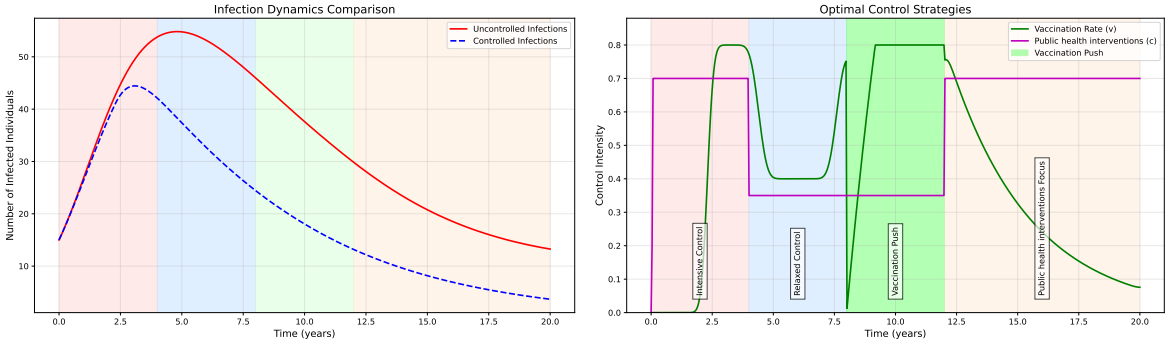

Figure 2: Infection dynamics under different control strategies (left) and corresponding intervention timeline (right).

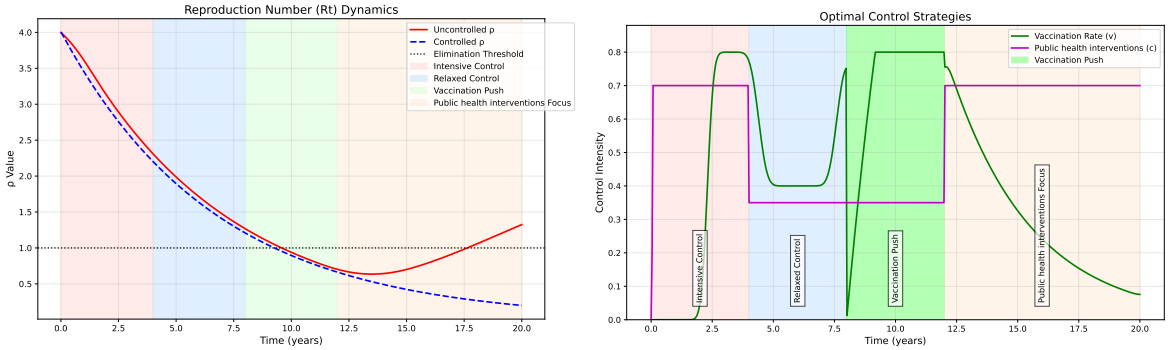

Figure 3: Evolution of the effective reproduction number (left) and control interventions timeline (right).

5.3. Economic Impact of Intervention Strategies

In addition to reducing infections, as indicated in Fig. 4 the proposed strategies support faster economic recovery. The simulated scenario with intervention recovers economically 25% faster than the uncontrolled case. Notably, public health actions implemented during the early and peak phases helped minimize long-term economic disruption. After year 12, the model shows limited fluctuation in economic output, attributed to a stabilized health situation and a decrease in control intensity.

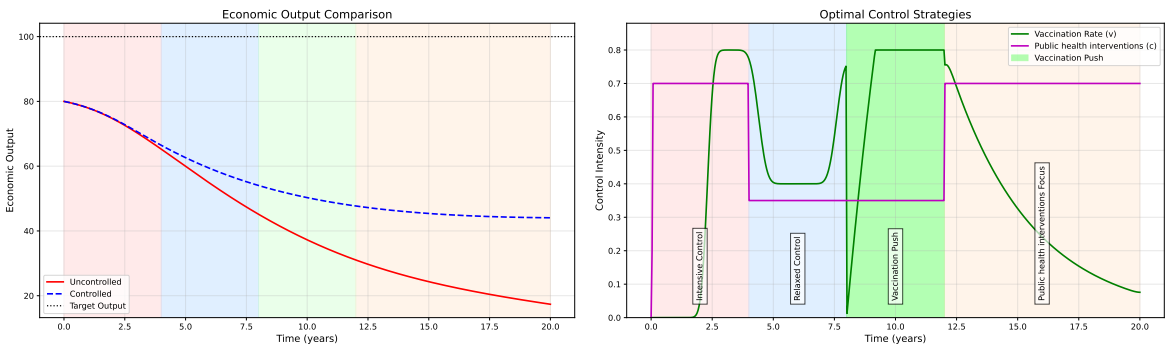

Figure 4: Economic output under different scenarios (left) and corresponding control strategy timeline (right).

5.4. Cost-Benefit Analysis

A comparative analysis of total costs in Fig. 5 indicates that the proposed control strategy is economically efficient. While the early phase of intervention demands substantial resources, the cumulative cost is 42% lower than the baseline by the end of the simulation. This is due to the long-term benefits of infection control, reduced mortality, and preserved economic productivity. The results support a strategy that balances health outcomes and economic stability.

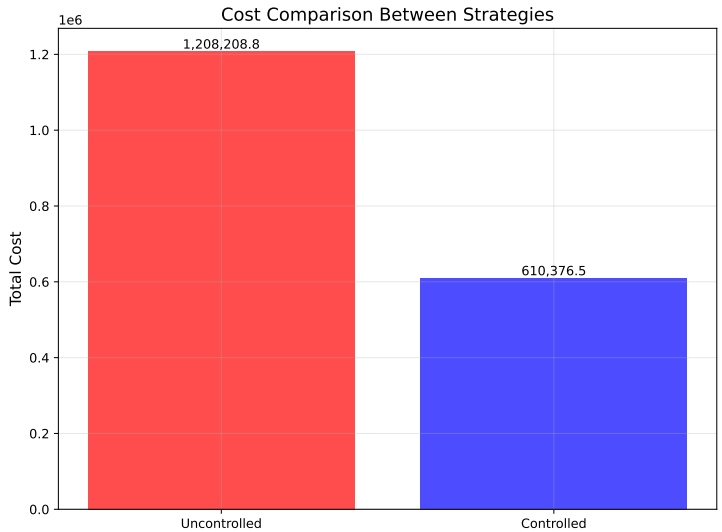

Figure 5: Total cost comparison between intervention and baseline scenarios.

5.5. Discussion

The SIRKρ framework generates dynamic intervention strategies that successfully balance epidemiological control with economic activity. The resulting optimal trajectories reveal a consistent three-phase pattern: an initial, intensive suppression of transmission using public health measures $c(t)$; a sustained vaccination effort $v(t)$ to build population immunity; and a final phase of adaptive interventions to prevent resurgence while minimizing economic disruption. This sequence emerges organically from the optimization process, not from predefined assumptions, suggesting it is a robust principle for reconciling short-term containment with long-term recovery.

Our model quantifies the non-linear trade-off between infection control and economic cost, confirming that early, decisive interventions, though costly upfront, avert greater long-term economic damage by preventing widespread transmission. This aligns with established findings where delayed action necessitates harsher, more costly corrections [1,12].

A key feature enabling this balance is the modeling of the effective reproduction number, $\rho(t)$, as a dynamic state variable. The terminal condition $\rho(T) \leq \rho_{\text{crit}}$ is crucial, as it ensures the epidemic is subcritical by the planning horizon's end, providing a rigorous foundation for a sustainable exit strategy by preventing the premature relaxation of controls.

While our experiments used HBV parameters, the quantitative results are specific to the chosen cost weights and model settings. The primary contribution is the adaptable framework itself, which can be tailored to other diseases, data contexts, and policy priorities. Future work could enhance its practical applicability by incorporating richer economic structures (e.g., sectoral costs) or accounting for uncertainty through robust or stochastic control.

Overall, the SIRKρ framework offers a structured basis for designing adaptive exit strategies. It allows authorities to move beyond cycles of rigid lockdowns and abrupt reopenings, instead using dynamic optimization to continuously adjust interventions based on real-time indicators. Our results demonstrate

that maintaining moderate, adaptable controls throughout a vaccination campaign yields superior long-term outcomes compared to the complete removal of restrictions.

6. Conclusion

The SIRKρ model presented in this study offers a significant advance in mathematical epidemiology by unifying the dynamics of disease transmission with economic impacts. Our framework extends traditional compartmental models through the incorporation of time-varying reproduction numbers and explicit economic feedback, enabling more realistic policy optimization. The analytical derivation of optimal control strategies using Pontryagin's Maximum Principle provides rigorous theoretical foundations for intervention design, while numerical simulations with HBV parameters demonstrate practical applicability.

Key findings reveal that the phased implementation of vaccination and public health measures can effectively control the spread of the disease while minimizing economic disruption. The model's ability to maintain the reproduction number below critical thresholds while accounting for economic costs represents an important contribution to both theoretical epidemiology and public health practice. These results suggest that integrated approaches considering both biological and socioeconomic factors can lead to more sustainable and effective outbreak response strategies.

Future research directions could explore model extensions to account for spatial heterogeneity, multi-strain dynamics, or behavioral adaptations. The flexibility of the framework allows for adaptation to various infectious diseases and public health contexts, making it a valuable tool for evidence-based policy making. The SIRKρ model ultimately bridges the gap between theoretical epidemiology and practical disease control, offering a robust platform to optimize intervention strategies in complex real-world scenarios.

A. Existence and Characterization of the Endemic Equilibrium

We derive the expressions for the endemic equilibrium of the reduced system (3.1). Thus, the steady-state equations are:

$$0 = \Lambda - (\mu + v)S^* - \rho^*\gamma\frac{S^*I^*}{N^*}, \tag{A.1}$$

$$0 = \rho^*\gamma\frac{S^*I^*}{N^*} - (\mu + \nu + \sigma)I^*, \tag{A.2}$$

$$0 = \eta - \alpha(\rho^* - \rho_0) - kI^* - \beta_v v - \beta_c c. \tag{A.3}$$

Theorem A.1 *For the system (A.1)-(A.3), there exists a unique endemic equilibrium*

$$E^* = (S^*, I^*, \rho^*), \qquad S^* > 0,\ I^* > 0,$$

if and only if the disease-free reproduction number satisfies

$$R_{\text{DFE}} > 1.$$

Proof: The proof proceeds in three steps: characterization, existence, and uniqueness.

1. Characterization. At equilibrium with $I^* > 0$, equation (A.2) implies

$$\rho^*\gamma\frac{S^*}{N^*} = \mu + \nu + \sigma. \tag{A.4}$$

From (A.1),

$$S^* = \frac{\Lambda - (\mu + \nu + \sigma)I^*}{\mu + v}, \qquad 0 < I^* < \frac{\Lambda}{\mu + \nu + \sigma}. \tag{A.5}$$

From (A.3),

$$\rho^* = \rho_0 + \frac{1}{\alpha}\Big(\eta - kI^* - \beta_v v - \beta_c c\Big). \tag{A.6}$$

Substituting (A.5) and (A.6) into (A.4) eliminates S^* and ρ^*, yielding a single scalar condition for I^*:

$$\mathcal{F}(I^*) := \rho^*(I^*)\,\gamma\,S^*(I^*) - (\mu+\nu+\sigma)\big(S^*(I^*)+I^*\big) = 0. \tag{A.7}$$

Thus, an endemic equilibrium corresponds to a root of $\mathcal{F}(I^*)$ in the interval

$$I^* \in \Big(0, \tfrac{\Lambda}{\mu+\nu+\sigma}\Big).$$

2. Existence. At the disease-free equilibrium (DFE), $I^* = 0$, we have

$$S_0 = \frac{\Lambda}{\mu+v}, \qquad \rho_{\mathrm{DFE}} = \rho_0 + \frac{1}{\alpha}\big(\eta - \beta_v v - \beta_c c\big). \tag{A.8}$$

The reproduction number is

$$R_{\mathrm{DFE}} = \frac{\rho_{\mathrm{DFE}}\gamma}{\mu+\nu+\sigma}. \tag{A.9}$$

Now evaluate $\mathcal{F}(I^*)$:

$$\begin{aligned}\mathcal{F}(0) &= S_0\big(\rho_{\mathrm{DFE}}\gamma - (\mu+\nu+\sigma)\big)\\ &= S_0(\mu+\nu+\sigma)(R_{\mathrm{DFE}}-1).\end{aligned} \tag{A.10}$$

Hence $\mathcal{F}(0) > 0 \iff R_{\mathrm{DFE}} > 1$.

At $I^*_{\max} = \frac{\Lambda}{\mu+\nu+\sigma}$, we have $S^* = 0$, so

$$\mathcal{F}(I^*_{\max}) = -(\mu+\nu+\sigma)I^*_{\max} = -\Lambda < 0. \tag{A.11}$$

Since $\mathcal{F}$ is continuous on $[0, I^*_{\max}]$, the Intermediate Value Theorem implies that if $R_{\mathrm{DFE}} > 1$, then $\mathcal{F}$ has at least one root in $(0, I^*_{\max})$. Thus, an endemic equilibrium exists.

3. Uniqueness. Substituting (A.5)–(A.6) into (A.7) shows that $\mathcal{F}(I^*)$ is quadratic:

$$\mathcal{F}(I^*) = A(I^*)^2 + BI^* + C, \tag{A.12}$$

with leading coefficient

$$A = \frac{k\gamma(\mu+\nu+\sigma)}{\alpha(\mu+v)} > 0. \tag{A.13}$$

Thus, $\mathcal{F}$ is concave-up. From Step 2, if $R_{\mathrm{DFE}} > 1$ then

$$\mathcal{F}(0) > 0, \qquad \mathcal{F}(I^*_{\max}) < 0. \tag{A.14}$$

Hence $\mathcal{F}$ has a unique root, which determines unique values of S^* and ρ^* via (A.5) and (A.6). This establishes the uniqueness of the endemic equilibrium. □

References

1. Acemoglu, D., Chernozhukov, V., Werning, I., Whinston, M. D. *Optimal targeted lockdowns in a multi-group SIR model*, NBER Working Paper 27102, (2020).
2. Balderrama, R., Peressutti, J., Pinasco, J. P., Vazquez, F., de la Vega, C. S. *Optimal control for a SIR epidemic model with limited quarantine*, Sci. Rep. 12(1), 12583, (2022).
3. Berestycki, H., Desjardins, B., Weitz, J. S., Oury, J.-M. *Epidemic modeling with heterogeneity and social diffusion*, J. Math. Biol. 86(4), 60, (2023).
4. Bouhmady, A., Serhani, M., Raissi, N. *Dynamic decision modeling for viable short- and long-term production policies: an HJB approach*, arXiv preprint arXiv:2509.12205, (2025).
5. Bouissa, A., Tahiri, M., Tsouli, N., Sidi Ammi, M. R. *Global dynamics of a time-fractional spatio-temporal SIR model with a generalized incidence rate*, J. Appl. Math. Comput. 69(6), 4779–4804, (2023).
6. Bouremani, T., Slimani, Y. *Optimal control of an SIR epidemic model based on dynamic programming approach*, J. Math. Sci., 1–14, (2024).

7. Cherkaoui-Dekkaki, O., Bouhmady, A., Benamara, I. *Multi-objective optimal control of a bioenergy–soil system under fertility constraints*, Nonlinear Science, 5, 100072, (2025).
8. Clarke, F. *Functional analysis, calculus of variations and optimal control*, Springer, vol. 264, (2013).
9. Del Valle, S. Y., Mniszewski, S. M., Hickman, K. S. *Modeling the impact of behavior changes on the spread of pandemic influenza*, Math. Biosci. Eng. 10(5–6), 1357–1374, (2013).
10. Diagne, M. L., Agusto, F. B., Rwezaura, H., Tchuenche, J. M., Lenhart, S. *Optimal control of an epidemic model with treatment in the presence of media coverage*, Sci. Afr. 24, e02138, (2024).
11. Federico, S., Ferrari, G., Torrente, M.-L. *Optimal vaccination in a SIRS epidemic model*, Econ. Theory 77(1), 49–74, (2024).
12. Ferguson, N. M., Laydon, D., Nedjati-Gilani, G. *Impact of non-pharmaceutical interventions (NPIs) to reduce COVID-19 mortality and healthcare demand*, Imperial College COVID-19 Response Team, (2020).
13. Flaxman, S., Mishra, S., Gandy, A., et al. *Estimating the effects of non-pharmaceutical interventions on COVID-19 in Europe*, Nature 584(7820), 257–261, (2020).
14. Fu, T., Li, S., Liu, M. *Dynamics and optimal control of an SIQR epidemic model with vaccination and individual feedback on networks*, J. Appl. Math. Comput., 1–18, (2025).
15. Funk, S., Gilad, E., Watkins, C., Jansen, V. A. A. *The spread of awareness and its impact on epidemic outbreaks*, Proc. Natl. Acad. Sci. 106(16), 6872–6877, (2010).
16. Gümüş, M., Türk, K. *Dynamical behavior of a hepatitis B epidemic model and its NSFD scheme*, J. Appl. Math. Comput. 70(4), 3767–3788, (2024).
17. Harko, T., Lobo, F. S. N., Mak, M. K. *Exact analytical solutions of the SIR epidemic model and of the SIR model with equal death and birth rates*, Appl. Math. Comput. 236, 184–194, (2014).
18. Hong, H. G., Li, Y. *Estimation of time-varying reproduction numbers underlying epidemiological processes: a new statistical tool for the COVID-19 pandemic*, PLoS One 15(7), e0236464, (2020).
19. Khan, T., Ullah, Z., Ali, N., Zaman, G. *Modeling and control of the hepatitis B virus spreading using an epidemic model*, Chaos Solitons Fractals 124, 1–9, (2019).
20. Kröger, M., Schlickeiser, R. *Analytical solution of the SIR-model for the temporal evolution of epidemics. Part A: time-independent reproduction factor*, J. Phys. A: Math. Theor. 53(50), 505601, (2020).
21. Kulenović, M. R. S., Nurkanović, M., Yakubu, A.-A. *Asymptotic behavior of a discrete-time density-dependent SI epidemic model with constant recruitment*, J. Appl. Math. Comput. 67(1), 733–753, (2021).
22. Pontryagin, L. S. *Mathematical theory of optimal processes*, Routledge, vol. 12, no. 1, 12583, (2018).
23. Saldaña, F., Korobeinikov, A., Barradas, I. *Optimal control against the human papillomavirus: protection versus eradication of the infection*, Abstr. Appl. Anal. 2019(1), 4567825, (2019).
24. Stanley, T. D., Doucouliagos, C., Jarrell, S. B. *Meta-regression analysis as the socio-economics of economics research*, J. Socio-Econ. 37(1), 276–292, (2008).
25. Suryanto, A., Kusumawinahyu, W. M., Darti, I., Yanti, I. *Dynamically consistent discrete epidemic model with modified saturated incidence rate*, Comput. Appl. Math. 32(2), 373–383, (2013).
26. Trélat, E. *Contrôle optimal: théorie & applications*, Vuibert Paris, vol. 36, (2005).
27. Weitz, J. S., Park, S. W., Eksin, C., Dushoff, J. *Awareness-driven behavior changes can shift the timing of epidemic peaks*, Nat. Commun. 11, 2608, (2020).
28. Yagasaki, K. *Optimal control of the SIR epidemic model based on dynamical systems theory*, Discrete Contin. Dyn. Syst.-B 27(5), 2501–2513, (2022).
29. You, C., Deng, Y., Hu, W., Sun, J., Lin, Q., Zhou, F., Pang, C. H., Zhang, Y., Chen, Z., Zhou, X.-H. *Estimation of the time-varying reproduction number of COVID-19 outbreak in China*, Int. J. Hyg. Environ. Health 228, 113555, (2020).
30. Zhou, S., Dai, Y., Wang, H. *Stability and Hopf bifurcation analysis of a networked SIR epidemic model with two delays*, J. Appl. Math. Comput. 71(1), 669–706, (2025).

ANLIMAD Team, LAMA Laboratory, Mohammed V University in Rabat, Rabat, Morocco
E-mail address: bouhmadiachraf@gmail.com

and

TSAN Team, TSI Laboratory, Faculty of SJES, Moulay Ismail University of Meknes, Morocco
E-mail address: m.serhani@umi.ac.ma

and

ANLIMAD Team, LAMA Laboratory, Mohammed V University in Rabat, Rabat, Morocco
E-mail address: nadia.raissi@fsr.um5.ac.ma